NEU PRESS

ASREL Aerospace Research Letters

Volume: 4 Issue: 1 Year: 2025 | Research Article | e-ISSN: 2980-0064

PID Design for Nonlinear Spacecraft Model with Reaction Wheels

Seda Nur ÇAKICI[1] Nur Sena KOCAKILIÇ[1] Amine El ARUK[1] Muhammet ÖZTÜRK[2*]

[1] Necmettin Erbakan University, Faculty of Aviation and Astronautics, Astronautical Engineering, Konya, Türkiye

[2] Necmettin Erbakan University, Faculty of Aviation and Astronautics, Aeronautical Engineering, Konya, Türkiye

Article Info

Received: 03.06.2025
Accepted: 17.06.2025
Published: 30.06.2025

Keywords:
Linearization,
PID,
Spacecraft dynamics,
Attitude control,
Reaction wheel.

ABSTRACT

The attitude control of a spacecraft is one of the most critical factors to ensure mission success. Satellites must maintain a constant orientation in space due to their operational objectives, such as communication satellites with directional antennas or those that depend on precise solar panel alignment to maximise energy efficiency. It is very important to keep the satellite stable at a predetermined position in space. To maintain this constant orientation and correct any disturbances, attitude control systems are used. The dynamics of such systems can be described using Newton's Second Law, which results in a set of non-linear equations for motion about the x, y and z axes. Due to their nonlinearity, these equations cannot be analysed directly using classical control methods based on transfer functions. PID (Proportional - Integral - Derivative) controllers are widely used in control systems, but their coefficients need to be determined appropriately. To obtain a suitable set of PID coefficients for satellite control via reaction wheels, the nonlinear system must first be linearised around a point close to the reference values. This ensures that the linear approximation accurately represents the system dynamics near the desired direction. This study aims to determine PID coefficients with respect to our desired control performance criteria. For this, the PID coefficients are calculated from the linearised system and applied to the original nonlinear model. For this calculation, the previously obtained linear model and actuator models are used. The PID coefficients are calculated by considering the desired settling time and overshoot. The PID coefficients are tested for linear and nonlinear models in simulation to show the effectiveness of the proposed approach.

Tepki Tekerlekli Doğrusal Olmayan Uzay Aracı Modeli için PID Tasarımı

Makal Bilgisi

Geliş Tarihi: 03.06.2025
Kabul Tarihi: 17.06.2025
Yayın Tarihi: 30.06.2025

Anahtar Kelimeler:
Lineerleştirme,
PID,
Uzay aracı dinamiği,
Yönelim control,
Reaksiyon tekeri.

ÖZET

Uzay aracının, özellikle uyduların yön kontrolü, görevin başarısını sağlamak için en kritik faktörlerden biridir. Uydular, yönlü antenlere sahip iletişim uyduları veya enerji verimliliğini en üst düzeye çıkarmak için hassas güneş paneli hizalamasına bağlı olanlar gibi operasyonel hedefleri nedeniyle uzayda sabit bir yönelimini korumak zorundadır. Uyduyu uzayda önceden belirlenmiş bir konumda sabit tutmak çok önemlidir. Bu sabit yönelimi korumak ve herhangi bir bozulmayı düzeltmek için yönelim kontrol sistemleri kullanılır. Bu tür sistemlerin dinamiği Newton'un İkinci Yasası kullanılarak tanımlanabilir ve bu da x, y ve z eksenleri etrafındaki hareket için bir dizi doğrusal olmayan denklemle sonuçlanır. Doğrusal olmamaları nedeniyle, bu denklemler transfer fonksiyonlarına dayalı klasik kontrol yöntemleri kullanılarak doğrudan analiz edilemez. PID (Oransal – İntegral - Türev) kontrolcüleri kontrol sistemlerinde yaygın olarak kullanılır, ancak katsayılarının uygun şekilde ayarlanması gerekir. Reaksiyon tekerlekleri aracılığıyla uydu kontrolü için uygun bir PID katsayıları kümesi elde etmek için, doğrusal olmayan sistemin önce çalışma noktasına yakın bir değer etrafında doğrusal hale getirilmesi gerekir. Bu durum, doğrusal yaklaşımın istenen yönelim yakınındaki sistem dinamiklerini doğru bir şekilde temsil etmesini sağlar. Bu çalışma, reaksiyon tekerlekleri ve doğrusal hale getirilmiş sistem modeli kullanarak uydular için optimal PID tabanlı bir yönelim kontrol sistemi geliştirmeyi amaçlamaktadır. Bunun için, PID katsayıları doğrusal hale getirilmiş sistemden hesaplanarak orjinal doğrusal olmayan modele uygulanır. Bu hesaplama için önceden elde edilen doğrusal model ve eyleyici modelleri kullanılmaktadır. İstenen oturma zamanı ve aşım değerleri göz önünde buludurularak PID katsayıları hesaplanmaktadır. Hesaplanan PID değerleriyle çalıştırılan simülasyonlar, kontrolcünün düşük aşım ve minimum hata ile kararlı bir performans elde ettiğini göstermektedir. Sonuçlar, bu yöntemin verimli uzay aracı yönelim kontrolü için etkinliğini doğrulamaktadır.

To cite this article:

Çakıcı, S. N., Kocakılıç, N. S., El Aruk, A. & Öztürk, M. (2025). PID design for nonlinear spacecraft model with reaction wheels. *Aerospace Research Letters (ASREL), 4*(1), 116-130. https://doi.org/10.56753/ASREL.2025.1.8

***Corresponding Author:** Muhammet Öztürk, *mozturk@erbakan.edu.tr*

INTRODUCTION

The attitude control of a spacecraft, particularly for satellites, is one of the most critical factors for ensuring mission success. Satellites often need to maintain a fixed orientation in space due to their operational objectives such as communication satellites with directional antennas or those that rely on precise solar panel alignment to maximize energy efficiency. So, attitude control is extensively studied in the literature because it is essential to keep the satellite stable at a predetermined position in space (He & Wu, 2021).

To maintain this fixed orientation and correct any disturbances, attitude control systems are employed. These systems often use active control mechanisms such as reaction wheels, gyroscopes, thrusters, or magnetorquers. The dynamics of such systems can be described using Newton's Second Law, resulting in a set of nonlinear equations for motion about the x, y, and z axes. Due to their nonlinearity, it is a challenge to overcome the control problems effectively (Kuznetsov et al., 2022).

PID (Proportional-Integral-Derivative) controllers are widely used in control systems, but they require appropriate determination of their coefficients (Borase et al., 2020; Çopur et al., 2024). Conventional PID coefficients determination methods, such as Ziegler-Nichols, Modified Ziegler-Nichols, Tyreus-Luyben, and the method proposed by Astrom and Hagglund, do not always provide optimal performance across different systems (Köprücü & Öztürk, 2024). Besides, these methods need linear systems to determine the PID coefficients.

There are many control studies for spacecraft attitude control in open literature. As an alternative to PID, Fuzzy Logic controller, adaptive fuzzy logic controller and Fuzzy tuned PID are tested and compared to classic PID controller (Shan et al., 2022; Calvo et al., 2016; Prajapat & Mandloi, 2014). Although the Fuzzy and adaptive Fuzzy controllers are more effective than conventional PID in terms of error minimization and response time, they tend to consume more energy, which is a significant drawback in space applications where power is limited, and efficiency is vital. Besides, they must be within a certain operating range of the system to operate at high performance. The PID coefficients are optimized by Genetic Algorithms to reach best performances (Daw et al., 2017). It is seen that the Genetic algorithm optimizes the system with respect to the control performance parameters such as minimizing the settling time, rise time etc. However, it is much easier to perform analytical calculations for linear systems when a certain performance of control is desired. Sliding Mode Control (SMC) based approaches are tested for attitude control by Chen and it is seen that the SMC is superior to classical PID controllers (Chen & Hu, 2022). But it is seen in the open literature that the SMC approaches must overcome chattering problem, so new approaches like Super Twisting SMC should be tested for the attitude control structures.

To obtain analytically a set of suitable PID coefficients for satellite control via reaction wheels for desired performance criteria, the nonlinear system must first be linearized around a value close to the operating point. This ensures that the linear approximation accurately represents the system's dynamics near the desired orientation (Moldabekov et al., 2023; Zhou, 2019).

In this paper, an optimal PID-based attitude control system is developed for satellites using reaction wheels and a linearized model. To obtain analytically a set of suitable PID coefficients for satellite control via reaction wheels for desired performance criteria, the nonlinear system must first be linearized around a value close to the operating point. This ensures that the linear approximation accurately represents the system's nonlinear dynamics around the linearization points (Moldabekov et al., 2023; Zhou, 2019). The PID coefficients are determined from the transfer function of the linearized system and then applied back to the original nonlinear model to evaluate performance in terms of stability and overshoot.

Within the scope of this study, PID coefficients that will provide the desired control performances for the nonlinear model of the spacecraft are analytically calculated and tested.

SPACECRAFT DYNAMICS

This section presents the analysis of a three-axis stabilized communication satellite employing momentum wheels for attitude control in the presence of small constant environmental torques. The satellite maintains a fixed orientation with respect to the Earth using internal torques generated by electric motors connected to flywheels. The satellites must have at least three reaction wheels for a 3-axis control if they are stated in the x, y, z axes (Curtis, 2019).

A momentum wheel is a spinning disk whose angular momentum can be varied by accelerating or decelerating the wheel via an electric motor. By Newton's third law, any change in the wheel's spin induces an equal and opposite torque on the spacecraft body. This internal exchange of angular momentum allows the spacecraft to reorient without expelling mass, unlike thrusters.

General mass equation:

$$m = m_o + \sum_{i=1} m_i \tag{1}$$

where m_0 is spacecraft body mass, m_i is mass of momentum wheels, m is total mass.

The total angular momentum of the spacecraft, H_G, of both the fuselage and the momentum wheels includes angular momentum.

The angular momentum equation:

$$H_g = H_{body} + \sum_{i=1}^{n} H_i \tag{2}$$

where H_i is angular momentum of momentum wheels, H_{body} is angular momentum of the spacecraft's body.

The angular momentum of each momentum wheel:

$$H_G^{(i)} = I_G^{(i)} \times w \tag{3}$$

Angular momentum of the spacecraft is given as:

$$H_G^{(body)} = I_G^{(body)} \times \omega \tag{4}$$

where H_G is total angular momentum of the spacecraft around its center of mass G, I_G is inertia tensor around the spacecraft's center of mass, w is angular velocity of the spacecraft's body.

If the spacecraft has asymmetry or different moments of inertia on different axes;

$$\begin{bmatrix} H_x \\ H_y \\ H_z \end{bmatrix} = \begin{bmatrix} I_x \times \omega_x \\ I_y \times \omega_y \\ I_z \times \omega_z \end{bmatrix} \tag{5}$$

The matrix form is expressed in this way:

$$H = \begin{bmatrix} Ixx & Ixy & Ixz \\ Iyx & Iyy & Iyz \\ Izx & Izy & Izz \end{bmatrix} = \begin{bmatrix} \omega x \\ \omega y \\ \omega z \end{bmatrix} \tag{6}$$

If no external torque is applied to the spacecraft, angular momentum is conserved.

$$\frac{dH_g}{dt} = 0 \tag{7}$$

- If it initially spins in a certain direction, it will continue to spin in that direction.
- If it's not spinning, it won't start spinning.
- This principle explains why objects moving in space (satellites and stations) maintain constant orientations, explains that it can hold or only gyroscopes, momentum flywheels, can change their direction.

If there is an external torque effect:

$$M = \frac{dH_G}{dt} = 0 \tag{8}$$

In this case, the angular momentum changes and the spacecraft turns to a different axis.

Spacecraft Orientation with Momentum Wheel

For objects moving in space, angular momentum is conserved because no external torque has no effect.

$$H_G = 0 \tag{9}$$

When the angular velocity of the momentum wheels is changed, the spacecraft reacts in opposite direction does

$$H_G = H_p + H_\omega \tag{10}$$

where H_ω is angular momentum of the spacecraft's body, H_P is angular momentum of momentum wheel, H_G is total angular momentum of the system.

Because the spacecraft and the momentum wheel are not initially moving.

$$\begin{bmatrix} H_\omega \\ H_p \end{bmatrix} = \begin{bmatrix} I_\omega \; x \; \omega_\omega \\ I_p \; x \; \omega_p \end{bmatrix} \tag{11}$$

Angular velocity of the spacecraft:

$$\omega_P = -\frac{I_\omega}{I_p}\omega_\omega \tag{12}$$

Integration of a DC Motor into the Momentum Wheel-Based Attitude Control System

In this study, a direct current (DC) motor is integrated into a spacecraft attitude control system that uses three momentum wheels mounted along the principal axes. The integration aims to enhance torque response and control authority, particularly on a selected axis. The DC motor operates with closed-loop feedback, using real-time data from onboard sensors like a star tracker to accurately apply torque and counteract external disturbances, ensuring stable spacecraft orientation

$$P(s) = \frac{\dot{\theta}(S)}{v(S)} = \frac{K}{(Js + b)(Ls + R) + K^2} \tag{13}$$

where:

b: Damping coefficient $\left(\frac{Nms}{rad}\right)$, models the frictional losses in the system that opposes motion

K: Engine constant $\left(\frac{Nm}{A}\right)$

J: Moment of inertia of the rotor(kgm^2), represents the resistance of the motor shaft to changes in angular velocity

L: Inductance represents the inertia to change in current in motor windings

R: Armature resistance, the electrical resistance of the motor windings

This transfer function represents the dynamic relationship between the input voltage $v(s)$ and the output angular velocity $\dot{\theta}(s)$ of a DC motor, expressed in the Laplace domain. It incorporates both the electrical and mechanical dynamics of the motor. These subsystems are coupled through the motor's torque constant K, which links electrical input to mechanical output.

The torque τ generated by the motor is related to angular velocity $\dot{\theta}(t)$ by:

$$\tau(t) = J\ddot{\theta}(t) + b\dot{\theta}(t) \tag{14}$$

The applied voltage $v(t)$ is used to overcome resistive, inductive and back-EMF effects.

$$v(t) = L\frac{di(t)}{dt} + R_i(t) + K\dot{\theta}(t) \tag{15}$$

where $K\dot{\theta}(t)$is the Back Electromotive Force (EMF) opposing in the input voltage. The torque is also directly proportional to the armature current:

$$\tau(s) = KI(s) \tag{16}$$

By applying Laplace transforms, the transfer function is obtained as:

$$\frac{\dot{\theta}(s)}{\vartheta(S)} = \frac{K}{(Js+b)(Ls+R)+K^2} \tag{17}$$

Satellite Inertia Tensor

The spacecraft has three identical momentum wheels. These wheels don't turn axes aligned with the spacecraft's primary body axes

$$I_G^{(v)} = \begin{bmatrix} A & 0 & 0 \\ 0 & B & 0 \\ 0 & 0 & C \end{bmatrix} \tag{18}$$

Inertia tensors of momentum wheels are:

$$\left[I_G^{(1)}\right] = \begin{bmatrix} I & 0 & 0 \\ 0 & 0 & 0 \\ 0 & 0 & 0 \end{bmatrix} \qquad \left[I_G^{(2)}\right] = \begin{bmatrix} 0 & 0 & 0 \\ 0 & J & 0 \\ 0 & 0 & 0 \end{bmatrix} \qquad \left[I_G^{[3]}\right] = \begin{bmatrix} 0 & 0 & 0 \\ 0 & 0 & 0 \\ 0 & 0 & J \end{bmatrix} \tag{19}$$

The angular velocities of the spacecraft in 3 axes $\omega_x, \omega_y, \omega_z$ and the momentum wheels are defined as $\omega^{(1)}, \omega^{(2)}, \omega^{(3)}$. Expression for total angular momentum H_G is written as follows:

$$\{H_G\} = \left[I_G^{(v)}\right]\{\omega\} + \sum_{j=1}^{3}\left[I_G^{\{v\}}\right]\left(\{\omega\} + \left\{\omega_{rel}^{(i)}\right\}\right) \tag{20}$$

This expression is simplified by substituting the inertia tensors and angular velocity values given above and is obtained in the following form:

$$\{H_G\} = \begin{bmatrix} A+I+2J & 0 & 0 \\ 0 & B+I+2J & 0 \\ 0 & 0 & C+I+2J \end{bmatrix}\{\omega\} + \begin{bmatrix} I & 0 & 0 \\ 0 & I & 0 \\ 0 & 0 & I \end{bmatrix} \cdot \begin{bmatrix} \dot{\omega}^{(1)} \\ \dot{\omega}^{(2)} \\ \dot{\omega}^{(3)} \end{bmatrix} \tag{21}$$

Solving the resulting equations for the angular accelerations of inertia wheels in 3 different axes then it is shown as below.

$$\begin{bmatrix} \dot{\omega}^{(1)} \\ \dot{\omega}^{(2)} \\ \dot{\omega}^{(3)} \end{bmatrix} = \begin{bmatrix} \frac{(M_G)_x}{I} + \frac{B-C}{I}\omega_y\omega_z - \left(1+\frac{A+2J}{I}\right)\dot{\omega}_x + \omega^{(2)}\omega_z - \omega^{(3)}\omega_y \\ \frac{(M_G)_y}{I} + \frac{C-A}{I}\omega_x\omega_z - \left(1+\frac{B+2J}{I}\right)\dot{\omega}_y + \omega^{(3)}\omega_x - \omega^{(1)}\omega_z \\ \frac{(M_G)_z}{I} + \frac{A-B}{I}\omega_x\omega_y - \left(1+\frac{C+2J}{I}\right)\dot{\omega}_z + \omega^{(1)}\omega_y - \omega^{(2)}\omega_x \end{bmatrix} \tag{22}$$

These equations cannot be directly used in system modelling due to their nonlinear nature. Therefore, it is necessary to first linearize the equations and then apply the Laplace transform. This process enables the derivation of the system's transfer function. A transfer function is defined, in linear systems with zero initial conditions, as the ratio of the Laplace transforms of the output function to that of the input function.

By setting the denominator of the transfer function equal to zero, the roots of the characteristic equation can be obtained. These roots are referred to as the poles of the system. If all poles have negative real parts, the system is considered stable; however, if even one pole does not have a negative real part, the system becomes unstable. For a system to be stable, all poles must lie on the left half of the complex plane.

DESIGN OF CONTROL PARAMETERS

In this paper, PID (Proportional-Integral-Derivative) control is applied, and to understand its implementation, it is important to first grasp the fundamental role of PID controllers in control systems. A PID controller continuously calculates the error between a desired setpoint and a measured process variable and then applies corrective actions based on three terms proportional, integral, and derivative to minimize this error. As reviewed by (Borase et al., 2020), PID controllers have been extensively studied due to their robustness and ease of application in both academic and industrial environments.

The PID control consists of three terms as proportional, integral and derivative terms.

The proportional term generates a control signal that is directly proportional to the current error. As the error increases, the controller's output increases proportionally, which enables fast and intuitive response.

Time domain $u_c(t) = k_P e(t)$

Laplace domain $U_c(s) = k_p E(s)$

The integral term eliminates steady-state errors by integrating the error over time. This ensures that even small errors are corrected cumulatively, resulting in a more accurate long-term response.

Time domain $u_c(t) = k_I \int_0^t e(\tau) d\tau$

Laplace domain $U_c(s) = \left[\frac{k_I}{s}\right] E(s)$

The derivative term forecasts future error behaviour by considering the rate of change of the error. This predictive action helps to dampen oscillations and reduce overshoots.

Time domain $u_c(t) = k_D \frac{de}{dt}$

Laplace domain $U_c(s) = [\,k_D s] E(s)$

In this study, the coefficients are first calculated manually after the nonlinear system is transformed into a linear approximation. The manually derived linear coefficients are then implemented back into the original nonlinear system to evaluate their performance. This approach allows observation of how the linear coefficients perform in a nonlinear context and to analyze the differences and effectiveness of this implementation.

System Linearization

The nonlinear system shown in the equations (23) is linearized. By focusing on an operating point around zero, the system's behavior is simplified, making the calculation of the PID coefficients easier. This step is essential for applying the PID controller effectively and improving the system's performance. The equation (23) can be written as:

$$\begin{bmatrix}\dot{\omega}_x\\ \dot{\omega}_y\\ \dot{\omega}_z\end{bmatrix}=\begin{bmatrix}\frac{(M_G)_x}{a}+\frac{B-C}{a}\omega_y\omega_z+\frac{I}{a}\omega^{(2)}\omega_z-\frac{I}{a}\omega^{(3)}\omega_y-\frac{I}{a}\dot{\omega}^{(1)}\\ \frac{(M_G)_y}{b}+\frac{C-A}{b}\omega_x\omega_z+\frac{I}{b}\omega^{(3)}\omega_x-\frac{I}{b}\omega^{(1)}\omega_z-\frac{I}{b}\dot{\omega}^{(2)}\\ \frac{(M_G)_z}{d}+\frac{A-B}{d}\omega_x\omega_y+\frac{I}{d}\omega^{(1)}\omega_y-\frac{I}{d}\omega^{(2)}\omega_x-\frac{I}{d}\dot{\omega}^{(3)}\end{bmatrix} \tag{23}$$

for $a = I + A + 2J$, $b = I + B + 2J$ and $d = I + C + 2J$

The Taylor series expansion is used to linearize the nonlinear system around zero. By retaining only the first order terms, a linear model is obtained which approximates the behavior of the system around zero.

$$T(x) \approx T(0) + \frac{dT}{dx}|_{x=x_0}(x - x_0) + \frac{dT}{du}|_{x=x_0}(u - u_0) \tag{24}$$

This linear approximation simplifies the system for controller design.

Under the assumption $\omega_0^{(1)} = \omega_0^{(2)} = \omega_0^{(3)} = \dot{\omega}_0^{(1)} = \dot{\omega}_0^{(2)} = \dot{\omega}_0^{(3)} = (M_G)_{x_0} = (M_G)_{y_0} = (M_G)_{z_0} = 0$

For first line in equation (23), the Taylor series expansion can be given as;

$$\begin{bmatrix} T_0\\ \frac{dT}{d\omega_y}|_{x=x_0}\\ \frac{dT}{d\omega_z}|_{x=x_0}\\ \frac{dT}{d(M_G)_x}\\ \frac{dT}{d\dot{\omega}^{(1)}}|_{x=x_0}\\ \frac{dT}{d\omega^{(2)}}|_{x=x_0}\\ \frac{dT}{d\omega^{(3)}}|_{x=x_0}\end{bmatrix}=\begin{bmatrix}\frac{B-C}{a}\omega_{y_0}\omega_{z_0}\\ \left(\frac{B-C}{a}\omega_z-\frac{I}{a}\omega^{(3)}\right)|_{x=x_0}=\frac{B-C}{a}\omega_{z_0}\\ \left(\frac{B-C}{a}\omega_z-\frac{I}{a}\omega^{(3)}\right)|_{x=x_0}=\frac{B-C}{a}\omega_{z_0}\\ \frac{1}{a}\\ -\frac{I}{a}\\ \frac{I}{a}\omega_z|_{x=x_0}=\frac{I}{a}\omega_{z_0}\\ -\frac{I}{a}\omega_{y_0}\end{bmatrix} \tag{25}$$

so;

$$\begin{aligned}\dot{\omega}_x = {}&\frac{B-C}{a}\omega_{y_0}\omega_{z_0} + \frac{B-C}{a}\omega_{z_0}(\omega_y - \omega_{y_0}) + \frac{B-C}{a}\omega_{y_0}(\omega_z - \omega_{z_0}) + \frac{I}{a}\omega_{z_0}\left(\omega^{(2)} - \omega_0^{(2)}\right)\\ &+ \frac{-I}{a}\omega_{y_0}\left(\omega^{(3)} - \omega_0^{(3)}\right) + \frac{-I}{a}\left(\dot{\omega}^{(1)} - \dot{\omega}_0^{-(1)}\right) + \frac{1}{a}(M_G)_x\end{aligned} \tag{26}$$

For $\omega_{x_0} = \omega_{y_0} = \omega_{z_0} = (M_G)_x = 0$;

$$\dot{\omega}_x = -\frac{I}{a}\dot{\omega}^{(1)} \tag{27}$$

For second line in equation (23), the Taylor series expansion can be given as;

$$\begin{bmatrix} T_0 \\ \frac{dT}{d\omega_x}|_{x=x_0} \\ \frac{dT}{dw_z}|_{x=x_0} \\ \frac{dT}{d\omega^{(1)}}|_{x=x_0} \\ \frac{dT}{dw^{(3)}}|_{x=x_0} \\ \frac{dT}{d\dot{w}^{(2)}}|_{x=x_0} \\ \frac{dT}{d(M_G)_y}|_{x=x_0} \end{bmatrix} = \begin{bmatrix} \frac{C-A}{b}\omega_{x_0}\omega_{z_0} \\ \frac{C-A}{b}\omega_{z_0} \\ \left(\frac{C-A}{b}\omega_x - \frac{I}{b}\omega^{(1)}\right)|_{x=x_0} = \frac{C-A}{b}\omega_{x_0} \\ -\frac{I}{b}\omega_{z_0} \\ \frac{I}{b}w_{x_0} \\ -\frac{I}{b} \\ \frac{1}{b} \end{bmatrix} \tag{28}$$

So;

$$\dot{\omega}_y = \frac{C-A}{b}\omega_{z_0}\omega_x + \frac{C-A}{b}\omega_{x_0}\omega_z - \frac{I}{b}\omega_{z_0}\omega^{(1)} + \frac{I}{b}\omega_{x_0}\omega^{(3)} - \frac{I}{b}\dot{\omega}^{(2)} + \frac{1}{b}(M_G)_y \tag{29}$$

For $\omega_{x_0} = \omega_{y_0} = \omega_{z_0} = (M_G)_y = 0$

$$\dot{\omega}_y = -\frac{I}{b}\dot{\omega}^{(2)} \tag{30}$$

For first line in equation (23), the Taylor series expansion can be given as;

$$\begin{bmatrix} T_0 \\ \frac{dT}{d\omega_x}|_{x=x_0} \\ \frac{dT}{d\omega_y}|_{x=x_0} \\ \frac{dT}{d\omega^{(1)}}|_{x=x_0} \\ \frac{dT}{d\omega^{(3)}}|_{x=x_0} \\ \frac{dT}{d\dot{\omega}^{(3)}}|_{x=x_0} \\ \frac{dT}{d(M_G)_{z_0}}|_{x=x_0} \end{bmatrix} = \begin{bmatrix} \frac{A-B}{d}\omega_{x_0}\omega_{y_0} \\ \frac{A-B}{d}\omega_{y_0} \\ \frac{A-B}{d}\omega_{x_0} \\ \frac{I}{d}\omega_{y_0} \\ \frac{-I}{d}\omega_{x_0} \\ -\frac{I}{d} \\ \frac{1}{d} \end{bmatrix} \tag{31}$$

so;

$$\dot{\omega}_z = \frac{A-B}{d}\omega_{y_0}\omega_x + \frac{A-B}{d}\omega_{x_0}\omega_y + \frac{I}{d}\omega_{y_0}\omega^{(1)} - \frac{I}{d}\omega_{x_0}\omega^{(2)} - \frac{I}{d}\dot{\omega}^{(3)} + \frac{1}{d}(M_G)_z \tag{32}$$

For $\omega_{x_0} = \omega_{y_0} = \omega_{z_0} = (M_G)_z = 0$

$$\dot{\omega}_z = -\frac{I}{d}\dot{\omega}^{(3)} \tag{33}$$

Calculation of PID Control Coefficients

Using the linearized system from the previous section, the PID coefficients were calculated manually to meet the desired system performance. Given the requirements of a 4 second settling time and 10% overshoot, the coefficients were determined as follows:

$$\mathrm{P.O} = 100e^{-\frac{\zeta\pi}{\sqrt{1-\zeta^2}}} = 10 \Rightarrow \zeta = 0.59 \tag{34}$$

$$T_s = \frac{4}{\zeta\omega_n} = 4 \Rightarrow \omega_n = 1.69 \tag{35}$$

Transfer function of the equation (27) can be written as;

$$G(s) = \frac{\omega_x(s)}{\omega^{(1)}(s)} = -\frac{I}{a} = -\frac{I}{I + A + 2J} = -\frac{1}{207} \tag{36}$$

where $I = 1, A = 200$ & $J = 3$.

The DC motor is also integrated into the system, which is represented by the following transfer function:

$$P(s) = \frac{\dot{\theta}(s)}{V(s)} = \frac{K}{(Js + b)(Ls + R) + K^2} = \frac{0.01}{0.05s^2 + 0.06s + 0.1001} \tag{37}$$

The PID control structure is given as:

$$G_c(s) = \frac{K_d s^2 + K_p s + K_i}{s} \tag{38}$$

Hence, the spacecraft system closed loop transfer function is determined as:

$$T(s) = \frac{G_c(s)P(s)G(s)}{1 + G_c(s)P(s)G(s)} \tag{39}$$

$$T(s) = \frac{-0.01\left(K_d s^2 + K_p s + K_i\right)}{10.35s^3 + (12.42 - 0.01K_d)s^2 + \left(20.72 - 0.01K_p\right)s - 0.01K_i} = \frac{{\omega_n}^2}{(10.35s + 2.07)(s^2 + 2\zeta\omega_n s + {\omega_n}^2)} \tag{40}$$

By comparing coefficients, the following values are obtained from equation (40):

$$\begin{bmatrix} K_p \\ K_i \\ K_d \end{bmatrix} = \begin{bmatrix} -5014 \\ -5912 \\ -2886 \end{bmatrix} \tag{41}$$

This method is used to obtain the PID coefficients for $\dot{\omega}_x$, can also be applied for $\dot{\omega}_y$ and $\dot{\omega}_z$. The linearized spacecraft system is constructed in the Simulink as given in Figure 1 and the determined control coefficients are implemented to the Simulink model as seen in Figure 2 to observe the control performance.

Afterwards, the calculated PID coefficients tested in nonlinear spacecraft system as shown in Figure 3 and Figure 4 to determine the control performances based on settling time, rise time, overshoot and Root Mean Square Error (RMSE).

Figure 1
Block Diagram of the Linear Control System

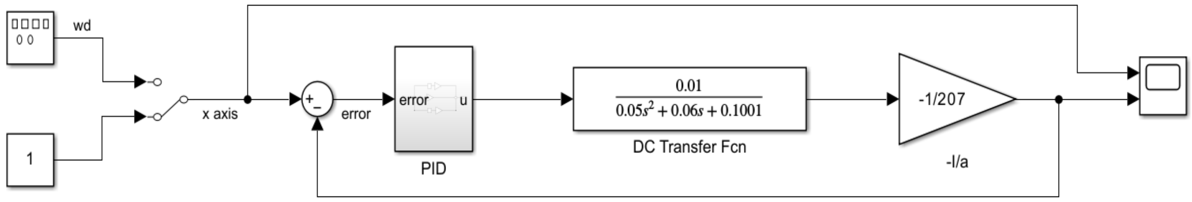

Figure 2
PID Structure

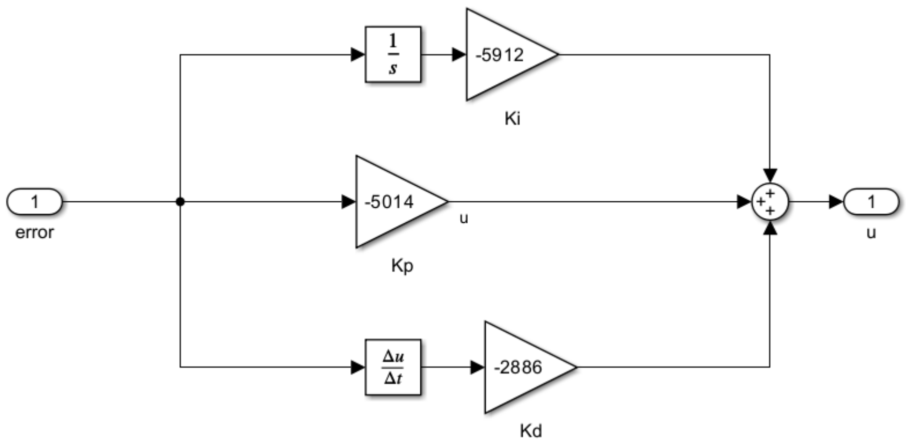

Figure 3
Block Diagram of the Nonlinear Control System

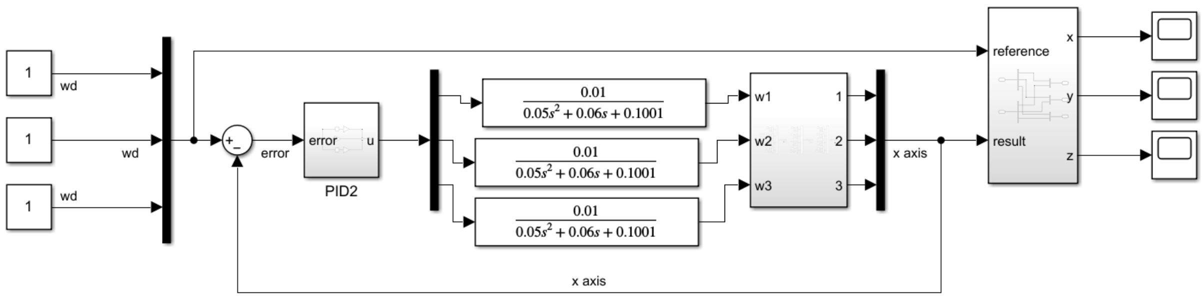

Figure 4
Block Diagram of the Nonlinear System

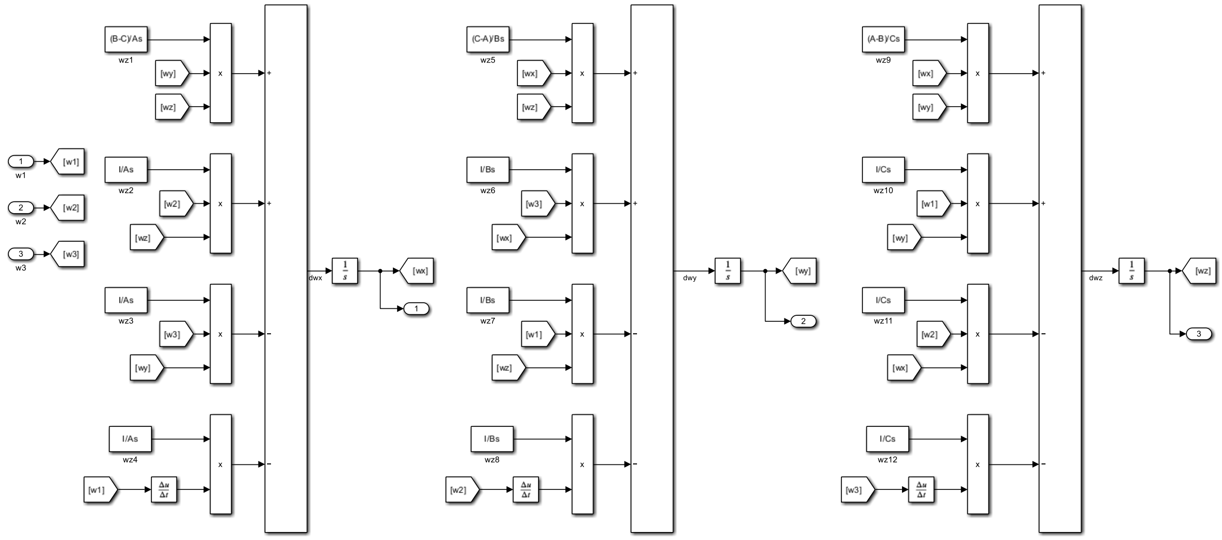

RESULTS

The PID controller coefficients derived from the linearized system were successfully implemented in both the linear and original nonlinear spacecraft models. Simulation results demonstrate that the closed-loop system approximately satisfies the desired performance criteria. As shown in Table 1, the linear model achieved a rise time of 0.7903 seconds, a settling time of 3.3236 seconds, and an overshoot of 21.324%, with a Root Mean Square Error (RMSE) of 4.61×10^{-5}. In contrast, the nonlinear model exhibited a slightly longer rise time of 0.9882 seconds and a settling time of 4.1679 seconds, but with a significantly lower overshoot of 4.1679% and a reduced RMSE of 1.558×10^{-5}.

Figure 5 illustrates the angular velocity responses of both the linear and nonlinear systems in comparison to the reference signal. It is observed that while the linear model reacts faster, it introduces a higher overshoot. The nonlinear model, although slightly slower, exhibits a smoother and more accurate convergence to the desired value.

These results confirm the successful application of the PID controller determined by using the linearized model. The nonlinear system benefits from enhanced stability and lower error. The comparison validates the practicality and effectiveness of applying PID coefficients derived from a linear approximation to a nonlinear spacecraft control scenario.

Table 1
Performance Comparison

System	Rising time	Settling time	Overshoot	RMSE
Linear Model	0.7903	3.3236	21.324	4.61×10^{-5}
Nonlinear Model	0.9882	4.1679	4.1679	1.558×10^{-5}

Figure 5

Control results of the nonlinear and linear system

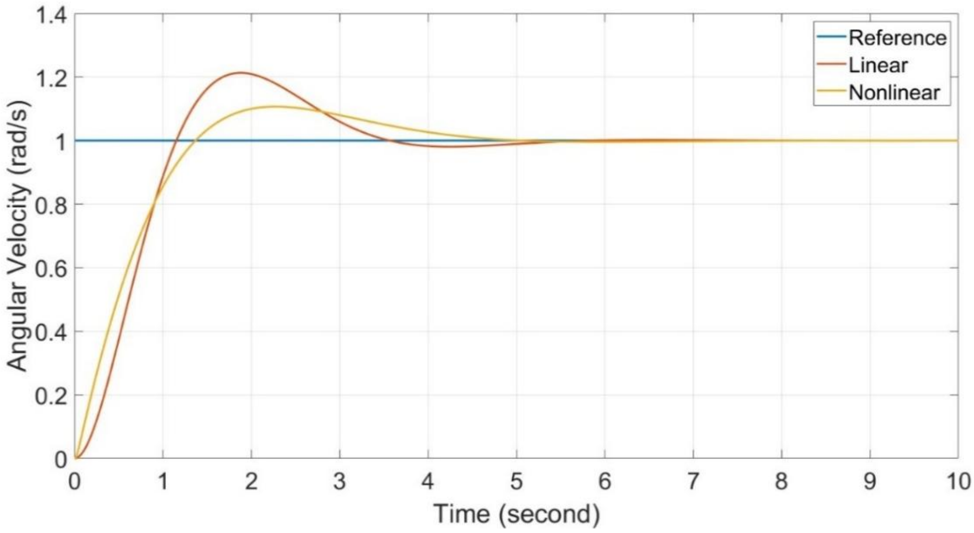

CONCLUSION

This study developed and implemented a PID-based attitude control system for a spacecraft equipped with reaction wheels. By linearizing the nonlinear dynamic equations around an operating point and calculating the PID coefficients from the resulting transfer function, the control system was designed to achieve a desired dynamic performance.

Simulation results demonstrated that the controller designed using the linear model performed effectively when applied to the original nonlinear system. While the linear model achieved faster response times, it resulted in higher overshoot. In contrast, the nonlinear model showed slightly longer settling and rising times but significantly lower overshoot and Root Mean Square Error (RMSE), indicating a more stable and precise system behavior.

In this study, these results confirm that PID control, when designed based on a linearized model, can be successfully applied to nonlinear spacecraft systems. The proposed method offers a practical and energy-efficient solution for satellite attitude control. This approach provides groundwork for future works with more complex systems.

Ethical Committee Approval

No human or animal subjects requiring ethical committee approval were used in this study. The research was conducted using publicly available data sets, literature reviews, or theoretical analyses. In accordance with ethical rules, full compliance with academic honesty and scientific ethical principles was maintained at every stage of the research process. Therefore, ethical committee approval was not required.

Author Contributions

Research Design (CRediT 1) Seda Nur ÇAKICI (20%) – Nur Sena KOCAKILIÇ (20%) – Amine El ARUK (20%) – Muhammet ÖZTÜRK (40%)

Data Collection (CRediT 2) Seda Nur ÇAKICI (25%) – Nur Sena KOCAKILIÇ (25%) – Amine El ARUK (25%) – Muhammet ÖZTÜRK (25%)

Research - Data Analysis - Validation (CRediT 3-4-6-11) Seda Nur ÇAKICI (20%) – Nur Sena KOCAKILIÇ (20%) – Amine El ARUK (20%) – Muhammet ÖZTÜRK (40%)

Writing of the Article (CRediT 12-13) Seda Nur ÇAKICI (20%) – Nur Sena KOCAKILIÇ (20%) – Amine El ARUK (20%) – Muhammet ÖZTÜRK (40%)

Text Revision and Improvement (CRediT 14) Seda Nur ÇAKICI (20%) – Nur Sena KOCAKILIÇ (20%) – Amine El ARUK (20%) – Muhammet ÖZTÜRK (40%)

Funding

There is no funding.

Conflict of Interest

There is no conflict of interest.

Sustainable Development Goals (SDG)

Sustainable Development Goals: 9 Industry, innovation and infrastructure

REFERENCES

Borase, R. P., Maghade, D. K., Sondkar, S. Y., & Pawar, S. N. (2021). A review of PID control, tuning methods and applications. *International Journal of Dynamics and Control, 9,* 818-827. https://doi.org/10.1007/s40435-020-00665-4

Calvo, D., Avilés, T., Lapuerta, V., & Laverón-Simavilla, A. (2016). Fuzzy attitude control for a nanosatellite in low Earth orbit. *Expert Systems with Applications, 58,* 102-118. https://doi.org/10.1016/j.eswa.2016.04.004

Chen, W., & Hu, Q. (2022). Sliding-mode-based attitude tracking control of spacecraft under reaction wheel uncertainties. *IEEE/CAA Journal of Automatica Sinica*, *10*(6), 1475-1487. https://doi.org/10.1109/JAS.2022.105665

Curtis, H. D. (2019). *Orbital mechanics for engineering students.* Butterworth-Heinemann.

Çopur, E.H., Bilgiç, H.H. & Ünler, T. (2024). Artificial intelligence based LQR and PID controller design of 3 degree of freedom system. *Necmettin Erbakan University Journal of Science and Engineering, 6(3),* 457-467. https://doi.org/10.47112/neufmbd.2024.58

Daw, M. S., Zayed, A. S., Allafi, N. I., & Husain, R. A. (2017). Genetic algorithm based PID controller for attitude control of geostationary satellite. *International Conference & Exhibition for Geospatial Technologies–Libya GeoTec,* 6-8 Nowember, 2, Tripoli, Libya, 318-330.

He, T., & Wu, Z. (2021). Iterative learning disturbance observer based attitude stabilization of flexible spacecraft subject to complex disturbances and measurement noises. *IEEE/CAA Journal of Automatica Sinica, 8(9),* 1576-1587. https://doi.org/10.1109/JAS.2021.1003958

Köprücü, S., & Öztürk, M. (2024). Comparison of PID coefficients determination methods for aircraft pitch angle control. *Aerospace Research Letters (ASREL), 3(1),* 15-26. https://doi.org/10.56753/ASREL.2024.3.5

Kuznetsov, N. V., Andrievsky, B., Kudryashova, E. V., & Kuznetsova, O. A. (2022). Stability and hidden oscillations analysis of the spacecraft attitude control system using reaction wheels. *Aerospace Science and Technology*, *131*, 107973. https://doi.org/10.1016/j.ast.2022.107973

Moldabekov, M., Sukhenko, A., Orazaly, Y., & Aden, A. (2023). Dynamics Analysis of a Nonlinear Satellite Attitude Control System Using an Exact Linear Model. *Mathematics, 11(12),* 2614. https://doi.org/10.3390/math11122614

Prajapat, P., & Mandloi, A. (2014). Performance Analysis of Fuzzy PID Controller Response. *International Journal of Advanced Research in Electrical, Electronics and Instrumentation Engineering.3(9),* 12208-12216. https://doi.org/10.15662/ijareeie.2014.0309070

Shan, Y., Xia, L., & Li, S. (2022). Design and simulation of satellite attitude control algorithm based on PID. In *Journal of Physics: Conference Series 2355(1)* 1-8. https://doi.org/10.1088/1742-6596/2355/1/012035

Zhou, B. (2019). On stability and stabilization of the linearized spacecraft attitude control system with bounded inputs. *Automatica, 105,* 448-452. https://doi.org/10.1016/j.automatica.2019.03.011